

Sensoric properties of aromatic and heterocyclic compounds with conjugated bonds^{*}

O. SALYK^{1**}, P. BEDNÁŘ¹, M. VALA¹, J. VYŇUCHAL²

¹Brno University of Technology, Faculty of Chemistry, Purkyňova 118, Brno

²Research Institute of Organic Syntheses, Rybitvi 296, Rybitvi, 533 54, Czech Republic

Dipyridyldiketopyrrolopyrrole and phenylpyridyldiketopyrrolopyrrole were investigated in terms of the effect of acid vapour on their properties, in comparison with diphenyldiketopyrrolopyrrole. Materials were deposited by vacuum evaporation in the form of thin films ca. 100 nm thick. Reversible changes of UV-VIS absorption spectra as well as those of IR absorption spectra when treated with acid vapour were tested. The explanation for the protonation of the ternary nitrogen atom in the pyridyl ring was found. The conductivity measured in a gap electrode arrangement increased by 5 to 6 orders of magnitude. All changes remained stable, unless the sample was regenerated by annealing at 170 °C and the entire process was fully reversible. The compounds exhibit good thermal and chemical stability and are suitable as detector materials in sensors of acids, vapours, and hydrogen.

Key words: *dipyridyldiketopyrrolopyrrole; UV-VIS spectra; IR spectra; conductivity*

1. Introduction

The future expectation of the hydrogen based economy will necessitate a vast demand for devices that operate on hydrogen, including new sensors. The main drawback of modern sensors is the need for extra energy for hydrogen dissociation.

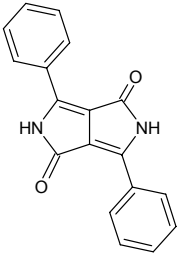
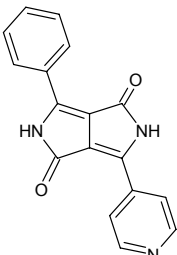
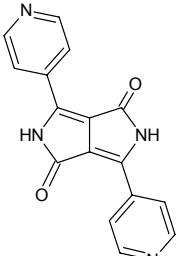
A comparative study of acid protonation of three diketopyrrolopyrrole (DPP) derivatives shown in Table 1 was performed. Derivatives of DPP compounds are widely used as colorants in the paint industry, especially as red pigments for automobile top-coat paints of various tones. The compound 1,4 diketo-3,6-bis phenyl-pyrrolo-[3,4-c]pyrrole (U4), specified also as DPP Scarlet EK (manufacturer Ciba-Geigy, name

^{*}The paper presented at the 11th International Conference on Electrical and Related Properties of Organic Solids (ERPOS-11), July 13–17, 2008, Piechowice, Poland.

^{**}Corresponding author, e-mail: salyk@fch.vutbr.cz

– Iragazin DPP Scarlet EK) [1] or as the pigment Red255, is the simplest, from which the other compounds are derived.

Table 1. Series of investigated compounds with maximum thermal stability T_m

	<p>U4 1,4 diketo-3,6-bis phenyl-pyrrolo-[3,4-c]pyrrole (DPP) diphenyldiketopyrrolopyrrole $T_m > 300\text{ }^{\circ}\text{C}$</p>
	<p>U34 1,4 diketo-3-phenyl-6-(4'-pyridyl) pyrrolo-[3,4-c]pyrrole $T_m > 300\text{ }^{\circ}\text{C}$</p>
	<p>U35 1,4 diketo-3,6-bis (4' -dipyridyl) pyrrolo-[3,4-c]pyrrole (DPPP) dipyridyldiketopyrrolopyrrole $T_m > 220\text{ }^{\circ}\text{C}$</p>

In 1993, Mizuguchi [2] noticed a colour change in the colorant diketo-dipyridylpyrrolopyrrole (DPPP) when the pigment dispersed layer in polymer was prepared at higher temperatures. It was found that traces of protons evolving from the polymer matrix were captured by three-valent nitrogen. A range of organic molecules exist containing three-valent nitrogen atoms with a high proton affinity. In the case of diketopyrrolopyrrole derivatives with pyridyl, piperidyl or a morpholinyl ring, we obtain a pigment that can change colour after protonation [2]. These materials are also semiconductive, thus protonation can influence their conductivity. It has already been observed in the case of a pyridyl derivative [3]. The protonation itself is tested in acid vapours, because in an acid water solvent the shielding effect of water molecules prevents proton penetration to active centres in the DPP film. Protonation in real hydrogen gas is possible only after dissociation of hydrogen molecules. It proceeds on the catalyst surface of a noble metal such as platinum or palladium [3]. The presence of an

electric field promotes hydrogen dissociation, so the clusters of non-conductive catalyst layer between gap electrodes have to be fabricated. The catalyst can be sputtered, evaporated or galvanically electrodeposited using anodic alumina templates [4] or simply spread by Pd nanoparticle suspension.

The mechanism of enhancement of the material conductivity is based on the donor function of a protonated quaternary nitrogen in a pyridyl ring. The electron contributes to the conductivity after hydrogen capture. The process is reversible; thermal hydrogen evolution brings the conductivity back to a low value [5].

2. Experimental

A comparative study of acid protonation of three DPP derivatives shown in Table 1 was performed. The compound U04 (3,6-diphenyl-2,5-dihydro-pyrrolo[3,4-c]pyrrole-1,4-dione) is a commercial pigment. This sample was prepared according to previous work [6]. Synthesis of the derivative U35 (3,6-di-pyridin-4-yl-2,5-dihydro-pyrrolo[3,4-c]pyrrole-1,4-dione) was carried out in compliance with the patent literature [7].

Synthesis of 3-phenyl-6-pyridine-4-yl-2,5-dihydro-pyrrolo[3,4-c]pyrrole-1,4-dione [8–10] (U34 derivative) was carried out as follows: *tert*-amyl alcohol (165 ml) and 3 g (0.13 mol) of metallic sodium were charged into a 500 cm³ flask equipped with a stirrer, a reflux condenser, a thermometer and a nitrogen inlet. Metallic sodium was dissolved under the reflux in the presence of a catalytic amount of FeCl₃ (it takes approximately 2 h), whereupon 6.7 g (0.064 mol) of 4-cyanopyridine was added. After that, 15 g (0.064 mol) of pyrrolinone ester [11] (in small portions) was continuously added over a total time of 15 min. This mixture was stirred and refluxed for 2 h. The reaction suspension of U34 sodium salt was cooled to 60 °C, and 100 cm³ of methanol together with 10 cm³ of acetic acid were added to protolyze it. The dark red suspension was again refluxed for 1 h and then filtrated after cooling to room temperature. The filtrate cake was dispersed in 300 cm³ of methanol and refluxed again for 1 h. The final product was filtrated off, washed with 100 ml of methanol and hot water. Yield: 5.15 g (28%) compound U34. MS analysis of U34 gave $M = 289$; negative ion MS: $m/z = 288 [M + H]^+$, 100%. NMR: ¹H chemical shifts: 11.15 (2H, br. s, NH); 8.84 (2H, m, H-orto Py); 8.55 (2H, m, H-orto Ar); 8.35 (2H, m, H-meta Py); 7.65 (3H, m, H-meta + H-para Ar) ¹³C chemical shifts were not determined, due to a very low solubility of the sample.

Thin films of DPP derivative materials were prepared by vacuum evaporation. The compounds were available in a powder form. Products composed of heterocyclic rings without alkyl chains bonded to the molecule appear to be poorly soluble in organic solvents and they cannot be deposited from solutions. They exhibit, however, good thermal resistance against pyrolysis and can be sublimed. Substrates were selected in the following way: high resistivity silicon wafers were used for FTIR spectroscopy, quartz glass for optical measurement, and glazed alumina plates for electrical gap arrangement. The deposition of the active DPP layer was carried out in a vacuum coat-

ing facility with the ultimate pressure of 1×10^{-4} Pa pumped by a diffusion oil pump. A crystal thin film thickness monitor was used for the deposition control. Thin films of 100 nm thickness were deposited on the selected substrates. The material was pressed into pellets 5.8 mm in diameter and about 1 mm high, typically having the mass of about 30 mg, which was the proper amount for producing a 200–300 nm thick layer without excess waste. The evaporator was home-designed in order to minimize possible decomposition, droplet creation, cluster sputtering, wastage and irradiation damage of the fabricated film. The shape of the molybdenum boat was optimized to focus the irradiation onto the pellet, thus it reduced the required heating power (Fig. 1). This procedure allowed a steady sublimation and deposition rate, without sputtering of bigger clusters or drops, in the case of non-melting material. It also improved ease of manipulation and general cleanliness—no powder was sputtered into a vacuum chamber. The thickness, checked by elipsometry, was typically 100 nm. The deposition rate was typically 0.2–0.5 nm/s. The 10 μ m gap was fabricated by aluminium contacts deposited by evaporation through a 10 μ m tungsten wire mask. (Fig. 2). Glazed corundum prefabricated substrates with firm gold contact layers for wire soldering and electrical shielding were used.

The samples were then analyzed using a scanning electron microscope (SEM) FEI QUANTA 200. No grain structure was observed at a scale of 50 nm resolution, so the surface appeared uniform. A NICOLET IMPACT 400 FTIR spectrometer was used for scanning IR spectra, and a Varian UV-VIS-NIR spectrometer was used for scanning UV-VIS spectra.

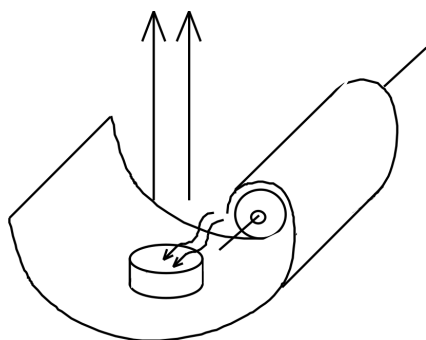


Fig. 1. Vacuum evaporation by radiative heating of the material pressed into a pellet

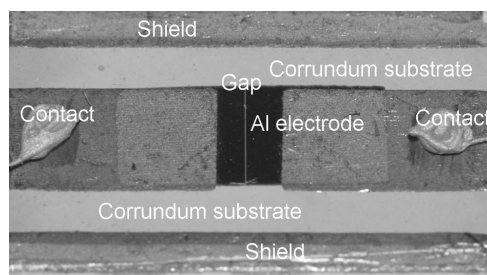


Fig. 2. Samples of DPP gap structure (10 μ m) on a glazed alumina plate with aluminium deposited contacts

3. Results and discussion

The effect of HNO_3 vapour treatment on thin film material was observed in changes of UV-VIS spectra, IR spectra and gap electrical conductivity. The investigated compounds (Table 1) in layers were first placed in a quartz cell and their absorbances in hydrochloric acid were measured. The attempt with acid aqueous solu-

tions of various pH brought only a weak spectral shift in the case of the U35 sample. It is explained by water molecules shielding protons, which means that the protons cannot penetrate into active centres of the film where they could be captured by quaternary nitrogen. Only acid vapours had a significant effect. Nitric and hydrochloric acids produced a very similar effect. Vapours of organic acids such as acetic acid and formic acid were tested and the results were similar but they damaged the layers by dissolving them quickly.

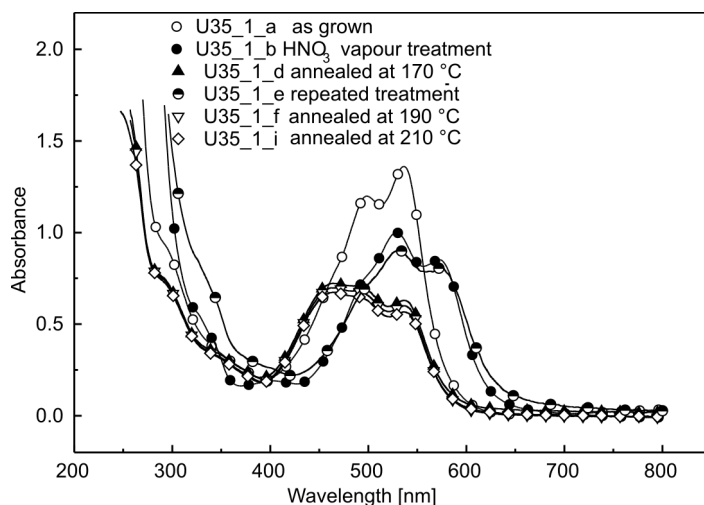


Fig. 3. Layer U-35. Absorption affected by vapour of nitric acid treatment and subsequent annealing

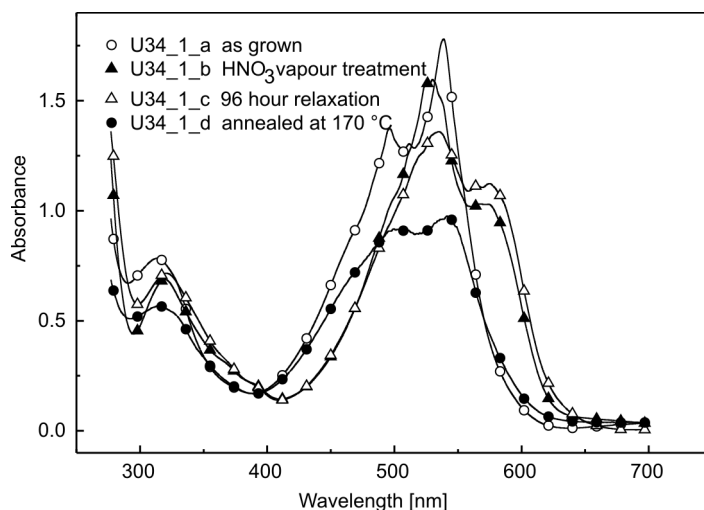


Fig. 4. Sample U34. Absorption affected by vapour of nitric acid treatment and subsequent annealing

Thin film samples of U34 and U35 react, in an etching dish, with HNO_3 vapour by changing their colour from vivid red to violet under the same conditions. A very similar reaction was observed in hydrochloric acid vapour. A U4 sample was taken as a reference with a similar absorption spectrum, where no detectable changes were observed.

Absorption spectra of thin film samples of U4, U34 and U35 on quartz glass substrates in the UV-VIS region were recorded. The results are presented in Figs. 3 and 4. The spectra of U4 sample are not presented, as they did not change in the presence of acid vapour. The effect proves that the quaternary nitrogen in the pyridyl ring is responsible for the absorbance variation. The nitric acid vapour treatment causes irreversible changes in the spectrum, which cannot be removed by the subsequent exposition to air – spectrum (b) in Fig. 3. This means that the acid vapour is firmly bonded and cannot be released at room temperature. Weak absorption decrease can be caused by pinhole damage in the layer or scratching. The annealing to 170°C leads to spectrum (d). A certain initial formation is present because the initial, as-grown layer spectrum (a) was not recovered. By repeated treatment and annealing, the recovered spectra switch between (b, d) and (e, f, i) regions and the effect is fully reversible if damages are negligible. Also the shape of the recovered spectrum differs from the initial one (a). This can be explained only by a structure change. The qualitative, permanent change in the U35 case (curves a–i) can be due to crystallographic dimorphism of the compound, as described by Mizuguchi et al. [3] and a change of the ratio of the amounts of the two phases by annealing. All thin films were also observed under a scanning electron microscope. The grain structure of $0.1\text{--}1\ \mu\text{m}$ with regular shapes as well as X-ray diffractograms are the evidence of crystallinity. These results will be presented elsewhere.

Sample U34 (Fig. 4) behaved very similarly, with the exception of a qualitative permanent change: the initial forming equivalent to thinning is observable but does not change the character of the spectrum. The acid treatment represents spectrum (b), the relaxation confirming stability for four days spectrum (c) and annealing change spectrum (d). It was then fully reversible and switched between curve (c) and (d) in Fig. 4 similarly as in the case of U35. X-ray diffractograms as well as the scanning electron microscopy show unimorphism.

The HNO_3 treatment also caused some changes in the IR absorption spectra. First, the U4, U34 and U35 samples were deposited with a thickness of $300\text{--}500\ \text{nm}$ on high resistivity silicon substrates. The comparison of their absorbances was related to maximum equal to 1 at $1640\ \text{cm}^{-1}$ corresponding to keto-oxygen bond and $1610\ \text{cm}^{-1}$ corresponding to N–H bond, which is also called amide II band [12]. These are the strongest absorption bands due to the largest electrical dipole moment in the molecule (Fig. 5). Substitution of the phenyl ring with the pyridyl ring has a slight effect on amide II band shift – single substitution in compound U34 from 1610 to $1595\ \text{cm}^{-1}$ and double substitution in compound U35 further to $1585\ \text{cm}^{-1}$. Other bands in the fingerprint region are weak due to smaller dipole moments and do not differ much for all three compounds. Only a small shift to lower energy oscillations with pyridyl substitution is apparent.

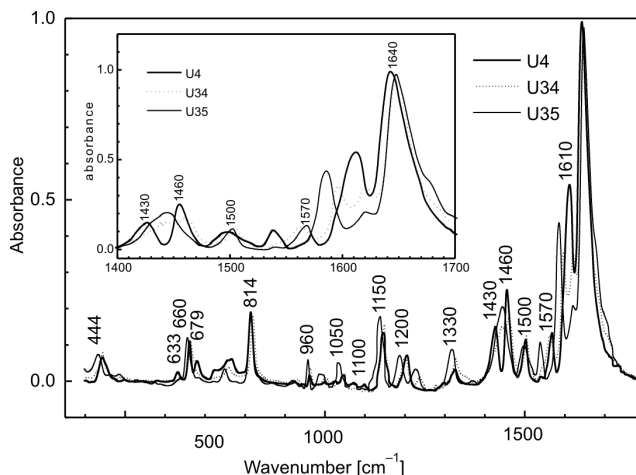


Fig. 5. IR spectra of compounds U4, U34 and U35

HNO_3 treatment of the U4 layer as a reference did not bring any visible changes in the IR spectrum. U34 layer showed significant increase of intensities of vibrational modes at 1320, 1460, 1500, 1530, 1630, and 1680 cm^{-1} as well as layer U35 even more considerable. This is explained by the higher dipole moment of the molecule when an N atom is charged by a proton and the remaining electron is captured in the central part of the molecule. A detailed analysis did not show any shift in the absorbance peak, as is apparent from Figs. 6, 7 but only their growth. This means that the oscillations are strengthened by charge redistribution and hence increase the electrical dipole moment in the molecule. In U35 case there appeared two strong new peaks at 1630 and 1680 cm^{-1} related to protonation which might have included weak peaks or shoulders at U34. This effect is not understood. The protonation – annealing process was fully reversible, as can be seen from the third spectrum scanned after recovery by annealing at 170 $^{\circ}\text{C}$.

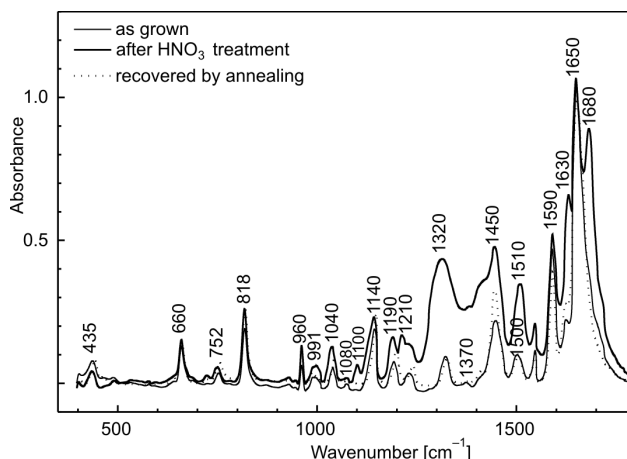


Fig. 6. Influence of HNO_3 treatment on IR absorption of U35 sample

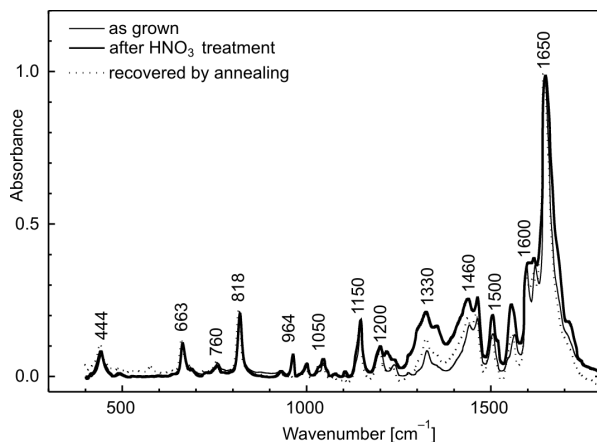


Fig. 7. Influence of HNO_3 treatment on IR absorption of U34 sample

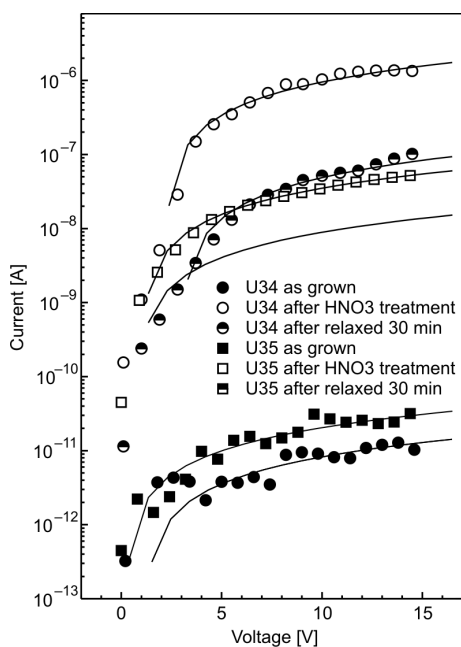


Fig. 8. Effect of HNO_3 treatment on conductivity of U34 and U35 samples

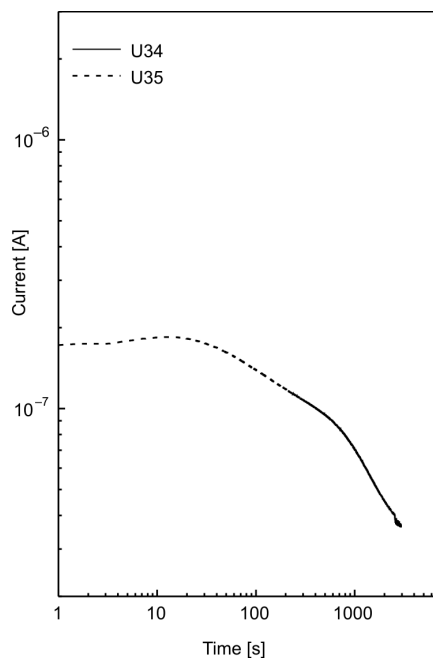


Fig. 9. Relaxation after acid vapour treatment under 4 V of voltage load

The conductivity and photoconductivity of thin films was tested as well since its changes under acid vapour treatment are expected. The measurements were carried out in the surface arrangement of electrodes, the inter-electrode distance amounting to 10 μm and the electrode lengths to 4 mm. The film thicknesses were equal to 100 nm. Voltages up to 15 V have been applied; the resulting current–voltage characteristics

were linear yielding the currents of the order of a few pA in the case of as grown films (cf. Fig. 8). This translates into specific conductivities of the order of $10^{-10} \Omega^{-1} \cdot \text{m}^{-1}$.

Repeated measurements after acid treatment proved irreproducible. The current permanently decreases as can be seen from the curves measured after 30 min relaxation. That is why the current was scanned at a constant applied voltage for a period of 3600 s. The current was found to decrease slow at first, as the carrier would be permanently supplied until exhaustion, and then a more rapid decrease is observed (Fig. 9). It gives evidence of more processes, affecting the current, such as decomposition of NO_3^- ion or quaternary nitrogen in pyridyl. The process is again reversible although small permanent forming changes appeared. No effect of the applied voltage on the relaxation process was observed.

The conductivity of U34 is higher than that of U35. We find it surprising as the U34 molecule has only one functional group. But full bonding saturation in the solid samples can play the role of some ternary nitrogen atoms. The latter could be already saturated by intermolecular interactions and not available for protons.

The explanation of reversible variations of properties proposed by Takahashi and Mizuguchi [2] may have the following explanation: one hydrogen ion from the acid is captured by the nitrogen atom in the pyridyl ring, and the complex salt $(\text{R}-\text{N}-\text{H})^+(\text{NO}_3)^-$ undergoes colour and structure change. The evolution of NO_2 and O_2 is possible as well, while the free electron remains in the material. In the case of dissociated hydrogen, it is presumed the reaction, where instead of $(\text{NO}_3)^-$ ion free electron is created, which contributes to material conductivity.

4. Conclusions

DPP pyridyl derivatives semiconductive organic pigments are able to capture protons in amine groups. HNO_3 vapour treatment offering protons leads to significant optical and electrical changes that are reversible. The dipole moment of the molecule is enhanced and increases the infrared absorption in the region $1230\text{--}1500 \text{ cm}^{-1}$. UV-VIS absorption exhibits significant growth of the absorption at 580 nm and decrease at 470 nm that results in a colour shift from red to violet. Absorption spectrum of the derivatives undergo hypsochromic shift. The protonation releases conductive electrons, thereby enhancing conductivity by orders of 10^{-10} to $10^{-6} \Omega^{-1} \cdot \text{cm}^{-1}$. Other side effect as conductivity, anomalous voltage-current characteristics and time relaxations were observed and will be further investigated. All processes described are reversible; the material can be recovered by annealing at 170°C and repeatedly tested. Relaxation tests indicate the presence of at least two processes with different time constants. It is believed that the studied derivatives can be exploited for the development of new sensing material, especially hydrogen sensing.

Acknowledgement

This work has been supported by the Czech Science Foundation in the projects GACR 203/08/1594 and by the Ministry of Industry and Trade of the Czech Republic via Tandem project No. FT-TA3/048).

References

- [1] SUZUKI E.M., J. Forensic Sci., 44 (1999), 297.
- [2] MIZUGUCHI J., Ber. Bunsenges Phys. Chem., 97 (1993), 684.
- [3] MIZUGUCHI J., TOMOHIKO I., TAKAHASHI H., YAMAMAKI H., Dyes Pigm., 68 (2006), 47.
- [4] KLOSOVÁ K., HUBÁLEK J., phys. stat. sol. (a), 205 (2008), 1435.
- [5] TAKAHASHI H., MIZUGUCHI J., J. Appl. Phys., 100 (2006), 034908.
- [6] VALA M., WEITER M., VYŇUCHAL J., TOMAN P., LUŇÁK S.JR., J. Fluoresc., 18 (2008), 1181.
- [7] ROCHAT A.C., CASSAR L., IQBAL A., US Pat. 4,579,949, (Ciba – Geigy Corporation 1983).
- [8] TAKAHASHI R., YAMAMOTO K., IQBAL A., HAO Z., Electrophotographic photoreceptor. Eur. Pat. Appl. (1996), 46 pp. CODEN: EPXXDW EP 718697 A2 19960626 CAN 125:181169 AN 1996:527278 CAPLUS.
- [9] MIZUGUCHI J., IQBAL A., GILLER G., Preparation of electrochromic diketopyrroles for electrochromic display devices. Ger. Offen. (1995), 10 pp. CODEN: GWXXBX DE 4435211 A1 19950427 CAN 123:83351 AN 1995:667261 CAPLUS.
- [10] ROCHAT A.C., CASSAR L., IQBAL A., 1, 4-Dioxopyrrolo [3,4-c] pyrroles. Eur. Pat. Appl. (1983), 32 pp. CODEN: EPXXDW EP 94911 A2 19831123 CAN 100:87260 AN 1984:87260 CAPLUS.
- [11] VYŇUCHAL J., LUŇÁK S.JR., HATLAPATKOVÁ A., HRDINA R., LYČKA A., HAVEL L., VYŇUCHALOVÁ K., JIRÁSKO R., Dyes Pigm., 77 (2008), 266.
- [12] WILLIAMS D.H., FLEMING I., *Spectroscopic Methods in Organic Chemistry*, McGraw-Hill, Maidenhead, Berks., UK, 1995.

Received 14 July 2008

Revised 28 November 2008